Biochem. Biophys. **282**, 275 (1990); L. G. Meszaros, I. Minarovic, A. Zahradnikova, *FEBS Lett.* **380**, 49 (1996); D. Stoyanovsky, T. Murphy, P. R. Anno, Y. M. Kim, G. Salama, *Cell Calcium* **21**, 19 (1997).
9. T. Aoki, T. Oba, K. Hotta, *Can. J. Physiol. Pharmacol.* **63**, 1070 (1985); T. Oba, M. Yamaguchi, S. Wang, J. D. Johnson, *Biophys. J.* **63**, 1416 (1992); T. Oba and K. Hotta, *Pflueg. Arch. Eur. J. Physiol.* **405**, 354 (1985); J. J. Abramson and G. Salama, *Mol. Cell. Biochem.* **82**, 81 (1988).
10. S. Lipton *et al.*, *Nature* **364**, 626 (1993); V. M. Bolotina, S. Najibi, J. J. Palacino, P. J. Pagano, R. A. Cohen, *ibid.* **368**, 850 (1994).
11. Canine cardiac SR vesicle fractions enriched in CRC activities were prepared in the presence of protease inhibitors [L. Xu, G. Mann, G. Meissner, *Circ. Res.* **79**, 1100 (1996)]. The CHAPS {3-[(3-cholamidopropyl)dimethylammonio]-1-propanesulfonate}-solubilized canine heart 30 S CRC complex was isolated by rate-density centrifugation. Gradient fractions were either concentrated by Centricon 30 (Amicon, Danvers, MA) centrifugation (to determine endogenous SNO levels) or reconstituted into proteoliposomes by removal of CHAPS by dialysis as described [H. B. Lee, L. Xu, G. Meissner, *J. Biol. Chem.* **269**, 13305 (1994)], except that the 20-hour dialysis buffer contained 10 mM potassium Pipes (pH 7.4), 0.25 M KCl, 10 μM EGTA, 20 μM Ca^{2+}, and 0.1 mM phenylmethylsulfonyl fluoride, and DTT was excluded from the buffers in some experiments. Protein concentrations were determined by using Amido Black [R. A. Kaplan and P. L. Pederson, *Anal. Biochem.* **150**, 97 (1985)].
12. S-Nitrosylation of the cardiac CRC was determined by a chemiluminescence assay as described in (*13*). Proteoliposomes containing the purified cardiac CRC (0.03 to 0.1 mg of protein per milliliter) were assayed either directly or after treatment for ~5 min at 24°C with various concentrations of GSNO, CysNO, or SIN-1 in 0.11 ml of buffer A [0.25 M KCl, 10 mM potassium Pipes (pH 7.4), and 10 μM free Ca^{2+} (10 μM EGTA and 20 μM Ca^{2+})]. NO donors were then removed by centrifugation through Sephadex G-25 spin columns equilibrated with buffer A. Mercury-displaceable SNO content was obtained by directly injecting one portion of the (flow-through) sample into the chemiluminescence instrument. Reversal of S-nitrosylation with DTT (10 mM DTT for 10 to 13 min at 24°C) was quantified by measuring the SNO content of the CRC after passage through Sephadex G-25 columns.
13. J. S. Stamler and M. Feelisch, in *Methods in Nitric Oxide Research*, M. Feelisch and J. S. Stamler, Eds. (Wiley, London, 1996), pp. 521–540.
14. Single channel measurements were performed at 23° to 25°C by fusing proteoliposomes containing the purified cardiac muscle CRC with Mueller–Rudin-type bilayers containing phosphatidylethanolamine, phosphatidylserine, and phosphatidylcholine in a 5:3:2 ratio (25 mg of total phospholipid per milliliter of *n*-decane) [L. Xu, G. Mann, G. Meissner, *Circ. Res.* **79**, 1100 (1996)]. The side of the bilayer to which the proteoliposomes were added was defined as the cis side. Single channels were recorded in a symmetric KCl buffer solution [0.25 M KCl and 20 mM potassium Hepes (pH 7.4)] containing 0.56 mM cis (SR cytosolic) EGTA and 0.50 mM cytosolic Ca^{2+} (2 μM free Ca^{2+}) and the additions described in the text. Electrical signals were filtered at 2 kHz, digitized at 10 kHz, and analyzed as described [L. Xu, G. Mann, G. Meissner, *Circ. Res.* **79**, 1100 (1996)].
15. G. Meissner, *Annu. Rev. Physiol.* **56**, 485 (1994)
16. L. Xu, A. H. Cohn, G. Meissner, *Cardiovasc. Res* **27**, 1815 (1993).
17. R. Radi, J. S. Beckman, K. M. Bush, B. A. Freeman, *J. Biol. Chem.* **266**, 4244 (1991); W. A. Pryor and G. L. Squadrito, *Am. J. Physiol.* **268**, L699 (1995); D. R. Arnelle and J. S. Stamler, *Arch. Biochem. Biophys.* **318**, 279 (1995); M. Feelisch and J. S. Stamler, in *Methods in Nitric Oxide Research*, M. Feelisch and J. S. Stamler, Eds. (Wiley, London, 1996), pp. 71–115; S. Mohr, J. S. Stamler, B. Brune, *FEBS Lett.* **348**, 223 (1994).
18. The free thiol content of the purified CRC reconstituted into lipid bilayer vesicles was determined by monobromobimane fluorescence [N. S. Kosower and E. M. Kosower, *Methods Enzymol.* **143**, 76 (1987)]. Control experiments showed no major interactions between monobromobimane (Calbiochem) and SNOs or the buffer. Background fluorescence of the proteoliposomes (and specificity of the bimane) was determined by derivatizing the reactive thiols with 14 μM $HgCl_2$ (*N*-ethylmaleimide derivatization gave comparable results) after which the mixture was passed through Sephadex G-25 spin columns and reacted with monobromobimane. Reactions were carried out with (100 μl) portions of proteoliposomes containing purified cardiac CRC (0.045 to 0.132 mg/ml) incubated with 50 μM monobromobimane protected from light for more than 1 hour at room temperature. Samples were then diluted to final volumes of 3 ml in quartz cuvettes and fluorescence intensities were measured at 482 nm with an excitation wavelength of 382 nm (Perkin-Elmer luminescence spectrophotometer LS50B). Standard curves were generated with known concentrations of monobromobimane-labeled glutathione mixed with the proteoliposomes.
19. K. Otsu *et al.*, *J. Biol. Chem.* **265**, 13472 (1990); J. Nakai *et al.*, *FEBS Lett.* **271**, 169 (1990).
20. E. Lam *et al.*, *J. Biol. Chem.* **270**, 26511 (1995).
21. B. Aghadasi, M. B. Reid, S. H. Hamilton, *ibid.* **272**, 25462 (1997).
22. P. C. Jocelyn, *Methods Enzymol.* **143**, 246 (1987); W. S. Allison, *Accounts Chem. Res.* **9**, 293 (1976).
23. H. F. Gilbert, *Adv. Enzymol.* **63**, 69 (1990); J. P. Ruppersberg *et al.*, *Nature* **352**, 711 (1991); R. J. Duhe *et al.*, *J. Biol. Chem.* **269**, 7290 (1994); R. Gopalakrishna, Z. H. Chen, U. Gundimeda, *ibid.* **268**, 27180 (1993); F. S. Sheu, C. W. Mahoney, K. Seke, K-P. Huang, *ibid.* **271**, 22407 (1996); K. A. Hutchinson *et al.*, *ibid.* **266**, 10505 (1991); Y. Dou *et al.*, *ibid.* **269**, 20410 (1994).
24. J. A. Thomas, B. Poland, R. Honzatko, *Arch. Biochem. Biophys.* **319**, 1 (1995); A. Hausladen, C. Privalle, J. DeAngelo, J. S. Stamler, *Cell* **86**, 719 (1996).
25. D. Simon, M. Mullins, H. Xu, D. Singel, J. S. Stamler, *Proc. Natl. Acad. Sci. U.S.A.* **93**, 4736 (1996).
26. P-F. Mery, S. M. Lohman, U. Walter, R. Fischmeister, *ibid.* **88**, 1197 (1991).
27. J. S. Stamler *et al.*, *Science* **276**, 2034 (1997).
28. Supported by grants from the National Institutes of Health to G.M. (HL 27430) and J.S.S. (HL52529 and HL59130). We thank D. A. Pasek for purifying the ryanodine receptor.

7 August 1997; accepted 24 November 1997

Functional Expression of a Mammalian Odorant Receptor

Haiqing Zhao, Lidija Ivic, Joji M. Otaki, Mitsuhiro Hashimoto, Katsuhiro Mikoshiba, Stuart Firestein*

Candidate mammalian odorant receptors were first cloned some 6 years ago. The physiological function of these receptors in initiating transduction in olfactory receptor neurons remains to be established. Here, a recombinant adenovirus was used to drive expression of a particular receptor gene in an increased number of sensory neurons in the rat olfactory epithelium. Electrophysiological recording showed that increased expression of a single gene led to greater sensitivity to a small subset of odorants.

Olfactory transduction begins with the binding of an odorant ligand to a protein receptor on the olfactory neuron cell surface, initiating a cascade of enzymatic reactions that results in the production of a second messenger and the eventual depolarization of the cell membrane (*1*). This relatively straightforward and common signaling motif is complicated by the existence of several thousand odorants, mostly low-molecular-weight organic molecules, and nearly a thousand different putative receptors (*2*, *3*). The receptors are believed to be members of the superfamily of G protein–coupled receptors (GPCRs) that recognize diverse ligands, including the biogenic amine neurotransmitters. Although the putative odorant receptors constitute the largest subfamily of GPCRs, in some ways they remain the most enigmatic, because no particular mammalian receptor has been definitively paired with any ligand. Functional expression of cloned odorant receptors would allow the characterization of the chemical receptive fields that provide the basis for coding and organization in the olfactory system.

A functional expression system for odorant receptors requires both that the receptors are properly targeted to the plasma membrane, and that they couple efficiently with a second messenger system that produces a measurable response to ligand stimulation. On the simple assumption that olfactory neurons themselves would be the most capable cells for expressing, targeting, and coupling odorant receptors, we have endeavored to use the rat nasal epithelium as an expression system, driving the expression of a particular receptor by including it in a recombinant adenovirus and infecting rat nasal epithelia in vivo. Here, we relied on the large number of putative odorant receptors, and their approximately equal expression among the 6 million neurons of the rat olfactory epithelium, to identify the average increase in response in an epithelium in which one of these receptors is overexpressed (*4*). This can be measured extracel-

H. Zhao, Interdepartmental Neuroscience Program, Yale University, New Haven, CT 06510, USA.
L. Ivic, J. M. Otaki, S. Firestein, Department of Biological Sciences, Columbia University, New York, NY 10027, USA.
M. Hashimoto and K. Mikoshiba, Molecular Neurobiology Lab, Tsukuba Life Sciences Center, RIKEN, Tsukuba, Ibaraki 305, Japan.
*To whom correspondence should be addressed.

lularly as a transepithelial potential resulting from the summed activity of many olfactory neurons, a measurement known as the EOG or electro-olfactogram (5). The amplitude of this voltage is determined by both the size of the response in individual cells and the number of cells responding.

Adenovirus vectors have been developed as a tool for efficient gene transfer in mammalian cells and have shown promise in a variety of experimental and clinical applications (6). We generated an adenovirus vector, AdexCAG-I7-IRES-GFP (Ad-I7) (Fig. 1A) (7), that contained an expression unit for a particular odorant receptor, rat I7 (2). This adenovirus vector is missing the E1 and E3 early genes, rendering it replication-incompetent and thereby preventing a lytic infection in treated olfactory epithelia (8). To aid in EOG electrode placement, we included the gene for the physiological marker green fluorescent protein (GFP) in the expression cassette, using an internal ribosomal entry site (IRES) insert to produce a bicistronic transcript that would result in the expression of odorant receptor and GFP as separate proteins in the same cells (9).

Animals were killed 3 to 8 days after infection (10) and the nasal cavity was opened, exposing the medial surface of the nasal turbinates (Fig. 1B). Under fluorescent illumination, the GFP clearly marked the pattern of viral infection and protein expression (Fig. 1, C and D). Expression was heterogeneous; in some regions of the epithelia as many as 20% of the cells were infected, whereas in others there was virtually no sign of infection. Overall, about 1 to 2% of the sensory neurons were infected and expressed the GFP gene product. There was significant variability between animals, with the highest infection rates often found in the second and third turbinates, usually near the edges (Fig. 1D). The reasons for these patterns of infectivity are not known, but the most likely explanation is simply access of the virus to tissue within the rather complex structures of the nasal cavity.

Expression of the bicistronic mRNA for the I7 receptor and GFP was verified by Northern blot of the infected epithelia (11). Using a probe that covered the entire coding sequence of the I7 gene, we detected a single band of about 2.8 kb in infected but not in uninfected epithelia, where native I7 expression is presumably below the level of detection (Fig. 1E). Although this does not provide a quantitative measure of the extent of mRNA expression in single cells, it does provide clear evidence that expression of the I7 receptor transcript is much higher in infected versus uninfected tissue. The high-gain signal amplification in olfactory neurons assures that even the activation of a few receptors by ligand will produce at least some sensory current in individual cells (12). In the absence of antibodies specific for the I7 odorant receptor, we used GFP antibodies (13) to further verify that

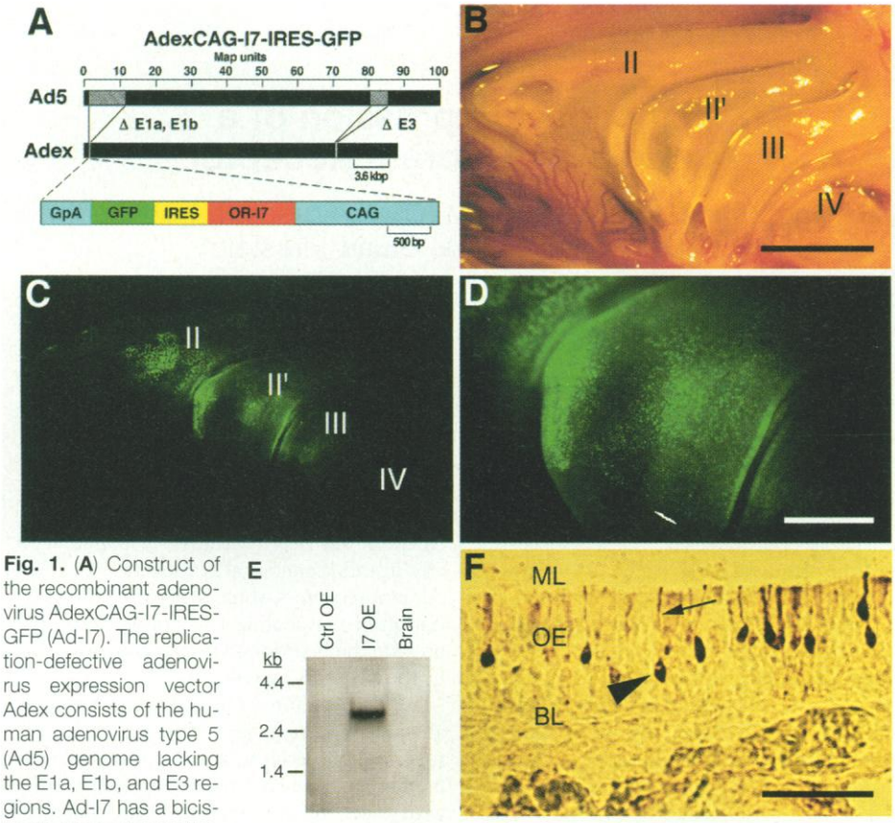

Fig. 1. (**A**) Construct of the recombinant adenovirus AdexCAG-I7-IRES-GFP (Ad-I7). The replication-defective adenovirus expression vector Adex consists of the human adenovirus type 5 (Ad5) genome lacking the E1a, E1b, and E3 regions. Ad-I7 has a bicistronic expression unit including the CAG promoter (CAG), odorant receptor I7 (OR-I7) coding sequence, internal ribosomal entry site (IRES), the S65T mutant of green fluorescent protein (GFP), and rabbit β-globin polyadenylation signal (GpA). The CAG promoter drives transcription of the bicistronic transcript I7-IRES-GFP, producing I7 odorant receptor and GFP as separate proteins. (**B**) Side view of the medial surface of the rat nasal turbinates. The turbinates are labeled with Roman numerals. Dorsal is up, anterior to the left. This animal was infected with Ad-I7 virus. (**C**) Fluorescent micrograph of the same tissue as in (B) showing the heterogeneous expression of GFP, which marked the location and the degree of virus infection. (**D**) Closer view of the Ad-I7 virus–infected endoturbinate II′ in (C). In regions of high fluorescence, we estimate that infection rates were near 10% of neurons. (**E**) Northern blot hybridization of total RNA from uninfected olfactory epithelia (Ctrl OE), Ad-I7 virus–infected olfactory epithelia (I7 OE), and rat brain with an I7 probe. A band of about 2.8 kb was detected in infected OE. This is near the expected size with the insert of 2.35 kb (I7-IRES-GFP) and 0.47 kb of untranslated sequence from the CAG promoter, and the β-globin polyadenylation signal sequence. Lanes were loaded with 20 μg of total RNA from each tissue. Examination of 28S and 18S ribosomal RNA confirmed the integrity of the RNA. (**F**) Cryosection (15 μm) of Ad-I7 virus–infected olfactory epithelium reacted with an antibody to GFP, showing stained olfactory neurons with characteristic morphology [including soma (arrowhead) and single dendrite (arrow)] and position within the olfactory epithelium. ML, mucous layer; OE, olfactory epithelium; BL, basal lamina. Scale bars, 3 mm [(B) and (C)], 1 mm (D), 50 μm (F).

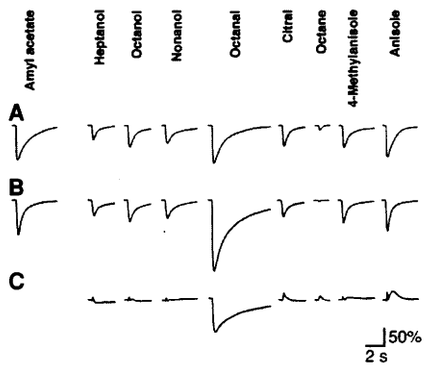

Fig. 2. Representative EOG recordings from an uninfected animal (**A**) and an Ad-I7 virus–infected animal (**B**). All EOGs are responses to odorants at a solution concentration of 10^{-3} M and are normalized to the reference odorant, amyl acetate, which is given the value of 1. (**C**) Subtraction of (A) from (B), which brings out the much-increased response to octyl aldehyde in the Ad-I7 virus–infected animal. The slight positive direction of some of the subtracted traces is primarily the result of differences in the time course of the responses in the different animals.

more than 80% of the infected cells were olfactory neurons (Fig. 1F). Thus, areas of high GFP fluorescence signal the positive infection of sensory neurons.

One difficulty in determining the ligand specificity of odorant receptors is the enormous stimulus repertoire to be tested. We developed a panel of 74 odorants, including aromatic and short-chain aliphatic compounds with various functional groups (*14*). Odorants were prepared by standard methods (*15*) and applied to the epithelium in the vapor phase by injecting a pressurized pulse of odor vapor into a continuous stream of humidified clean air. All odors were tested at a solution concentration of 10^{-3} to 10^{-2} M. Concentrations of stimulus at the olfactory epithelium could not be known, but the system reliably delivered the same amount of stimulus on each trial, as there was little variability between responses to successive pulses of the same odorant. The absolute odorant concentration at the tissue was not critical because it was the relative change in responsiveness between treated and untreated animals that was measured.

EOG recordings were obtained with a glass capillary electrode placed on the surface of the epithelium and connected to a differential amplifier (*16*). The EOG response is a negative-going spike of potential that is typically 0.5 to 15 mV in amplitude and 1.5 to 5 s in duration. To account for between-animal variability, we used a standard odorant, amyl acetate, to which all other odorant responses were normalized (*17*). EOGs were recorded from the region of olfactory epithelium that showed high numbers of fluorescent (infected) cells in Ad-I7 virus–infected turbinates; EOGs were also recorded in a similar location from uninfected animals. All infected animals were able to respond to all of the 74 odorants in the test panel, although responses to all odors in virally infected animals were on average 30% smaller in amplitude. Nonetheless, the amplitudes of the responses relative to the amyl acetate standard were unchanged. This was the only nonspecific effect attributable to the virus that we observed, and the same nonspecific reduction in response amplitude was also seen in animals infected with viruses containing only the *lacZ* or GFP genes.

Responses to eight representative odorants from the panel of 74 are shown for an

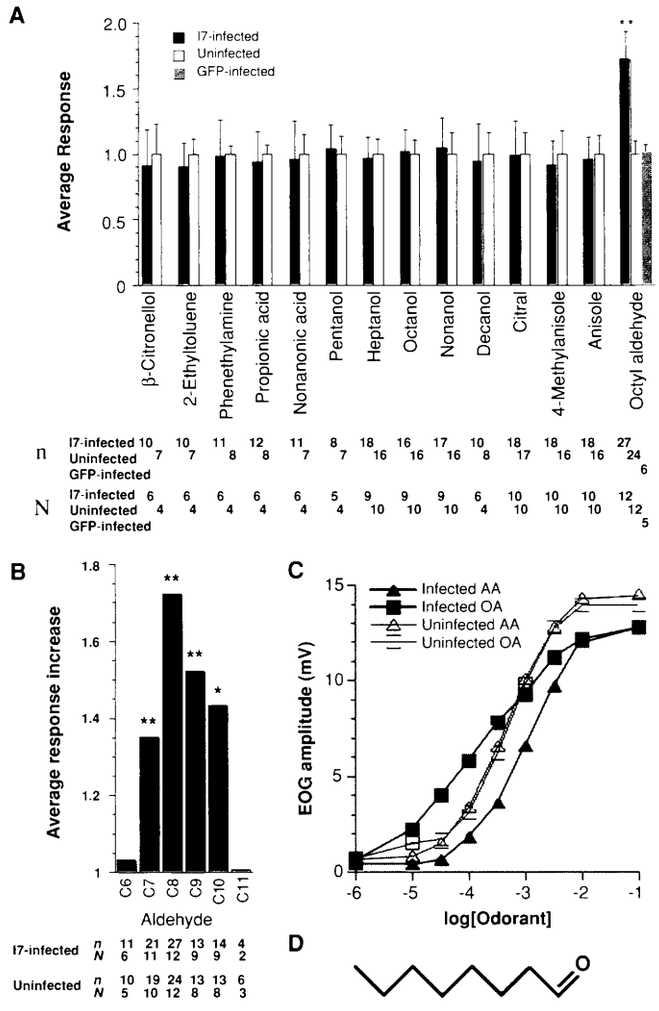

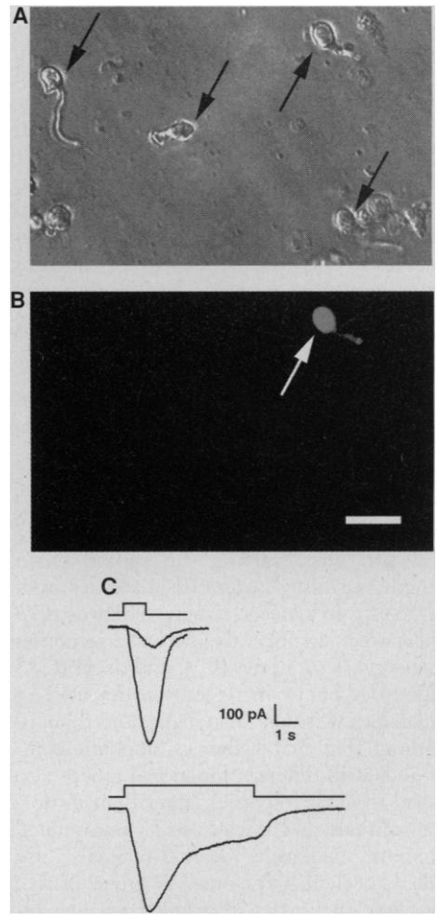

Fig. 3. (**A**) Comparison of average EOG amplitudes in Ad-I7 virus–infected and uninfected animals to 14 odorants at a solution concentration of 10^{-3} M (*n* = number of recordings, *N* = number of animals; error bars represent SD). All responses were normalized to the reference odorant, amyl acetate. Responses in uninfected animals are given the value of 1, and responses in infected animals are scaled accordingly. As a further control, the response to octyl aldehyde was compared with that in animals infected with an adenovirus carrying only GFP. Statistical significance of the data was evaluated with the *t* test (**$P < 0.001$). (**B**) I7 virus–infected animals have increased odorant responses to heptaldehyde (C_7), octyl aldehyde (C_8), nonyl aldehyde (C_9), and decyl aldehyde (C_{10}), but not to hexaldehyde (C_6) or undecylic aldehyde (C_{11}). The bars are the result of a subtraction that shows the relative increase of the average responses to these odorants in infected versus uninfected animals (*n* = number of recordings, *N* = number of animals). Statistical significance of the data was evaluated with the *t* test (**$P < 0.001$, *$P < 0.01$). (**C**) Comparison of responses (EOG amplitude) in an infected and uninfected animal to increasing concentrations of amyl acetate (AA, triangles) and octyl aldehyde (OA, squares). Heavy lines and solid symbols are from the infected animal; light lines and open symbols are from the uninfected control animal. The *x* axis is the logarithm of the molar concentration of odorant solutions. (**D**) The chemical structure of octyl aldehyde, $CH_3(CH_2)_6CHO$, variously described as having a light citrus, soapy, or fatty odor quality.

Fig. 4. (**A**) Freshly dissociated rat olfactory neurons (arrows) can be easily identified by their morphology. (**B**) In the same field under fluorescence illumination, an olfactory neuron infected by Ad-I7 virus can be identified by expression of GFP. Scale bar, 20 μm. (**C**) Sample whole-cell recordings from a GFP-positive cell. Top traces are responses to 5×10^{-4} M (larger) and 5×10^{-5} M (smaller) octanal; lower trace shows the response to a 6-s step of octanal at 10^{-4} M. Holding potential was −60 mV.

uninfected control animal and an animal infected with the Ad-I7 virus (Fig. 2). For seven of the eight odorants shown (plus the amyl acetate standard), as for 62 of the 65 other odorants in the panel, there was no appreciable change in responsiveness between the infected and uninfected animal. However, for one odorant—octyl aldehyde (octanal), an eight-carbon, straight-chain, saturated aliphatic aldehyde—the response was substantially greater, both in amplitude and time course, in the infected animal. The large increase in amplitude and time course indicated that more individual olfactory neurons were responsive to octyl aldehyde in the infected versus uninfected tissue.

The average response amplitudes for 14 of the odorants selected from the panel of 74, at a solution concentration of 10^{-3} M, were compared for both uninfected and Ad-I7–infected animals (Fig. 3A). Octyl aldehyde responses of infected animals were, on average, 1.7 times those of uninfected animals, whereas all other odorants were near control levels. The responses to octyl aldehyde were also compared with a control in which animals were infected with a virus containing only the GFP gene. Expression of GFP in these animals was comparable to that seen in animals infected with Ad-I7, but the response to octyl aldehyde was not different from uninfected animals. Thus, neither viral infection nor GFP was sufficient to generate the increase in responsivity to octyl aldehyde. Finally, the response increase was location-sensitive. If the EOG electrode was moved to an area with no GFP expression, the increased response to octanal was reduced to control levels.

We wished to determine if other, related odorants might also be recognized by the I7 receptor. First, varying the carbon chain length, we tested saturated aldehydes from C_3 to C_{12}. In addition to octyl aldehyde (C_8) there were significantly increased responses to heptyl (C_7), nonyl (C_9), and decyl (C_{10}) aldehydes, but no increases were detected for aldehydes with less than 7 or more than 10 carbons (Fig. 3B). Other C_8 aliphatic compounds with different functional groups also failed to elicit responses larger than in normal animals, and at least one C_8 unsaturated aliphatic aldehyde, *trans*-2-octenal, also failed to elicit a response. A group of five aromatic aldehydes also failed to give responses. Thus, the response profile of the I7 receptor, at least within the scope of the 74-odorant panel screened here, is relatively specific for C_7 to C_{10} saturated aliphatic aldehydes.

At the comparatively high concentrations used in these experiments, the response to octyl aldehyde in infected animals was on average 1.7 times the response in control animals. However, these high concentrations mask the full effect of the virally induced odorant receptor expression because of nonlinearities associated with high concentration responses. As can be seen in the dose-response relations (Fig. 3C), comparison of the octyl aldehyde response to the amyl acetate response at various concentrations revealed up to a sevenfold difference in response magnitude in the infected versus the uninfected epithelium. For example, at an odorant concentration of 5×10^{-5} M in solution, the response ratio of octanal to amyl acetate in the infected animal was 4.0:0.6 mV—a ratio of about 7. At the same concentration in the normal animal, the responses were nearly equal and the ratio was 1. Similar maximum increases, with response ratios ranging from 4 to 7, were measured in four infected animals.

Because the infected cells expressed GFP, it was possible to identify individual positive neurons after dissociation of the epithelium, allowing responses to be tested in single cells (Fig. 4). In whole-cell patch clamp recordings of single infected neurons, we recorded responses to octanal in each of seven GFP-positive cells (*18*). In uninfected cells we recorded a response to octanal in only 2 of 28 cells. The responses displayed latencies (150 to 250 ms) and amplitudes (90 to 500 pA) within the normal range (*12*), and both the kinetics and amplitude were concentration-dependent. Responses to maintained odor stimuli displayed a characteristic sag in the response, owing to adaptation (Fig. 4C). By these measures, the responses to octanal in virally transduced cells followed the pattern of normal odor responses in untreated cells, indicating that the endogenous second messenger system was most likely responsible for generating the response in the infected cells.

Thus, a member of the multigene family first identified as encoding putative odorant receptors (*2*) does indeed code for a protein that is capable of specific odor binding leading to a physiological response. On the basis of the controls, we believe that the increased octanal sensitivity in infected animals was not likely to have resulted from viral infection alone. Viral infection with either *lacZ* (*19*) or GFP viruses had no effect; the octanal response was selective for regions of the epithelium that had been infected; and the only nonspecific effect observed was a general reduction (by about 30%) in responsivity to all odors in infected epithelia.

Identifying the molecular receptive field of an olfactory sensory neuron is a critical first step in understanding how olfactory perception is achieved by higher brain centers. Within the limited set of odors tested, the I7 receptor is nonetheless striking in its ability to discriminate the C_6 hexanal, to which it shows no response, from the C_7 heptanal, which gives a strong response. Interestingly, to humans, hexanal has a grassy odor, whereas the C_7 to C_{10} aldehydes share a primarily fatty odor and the higher aldehydes have a stronger fruity or citrus quality. The chemical receptive field for this single odor receptor is similar to the response patterns recently measured in single olfactory neurons and in mitral cells of the olfactory bulb (*20*). One difference was that for mitral cells the carbon chain length appeared to be somewhat more critical than functional group in determining stimulus efficacy, whereas our results indicate that both are critical determinants. In an earlier report of odor receptor expression, the rat OR5 receptor, expressed by the baculovirus system in insect sf9 cells, showed a surprisingly wide-ranging sensitivity to odors from at least five separate chemical classes, all at low concentrations (*21*). This result is somewhat at odds with the data from mitral cell recordings and with our data, but it may be related to the expression system or the method of applying odor stimuli. Among nonmammalian odor receptors, the nematode receptor (ODR10) displayed a narrow ligand specificity (*22*), whereas three fish receptors responsive to a commercial fish food mixture have not been paired with specific ligands (*23*).

Genes of the odorant receptor subfamily have a hypervariable region corresponding to the second through fifth transmembrane domains (*2*), the presumed ligand-binding site in GPCRs (*24*). However, in some cases odorant receptors of the same subfamily differ from each other by only a few residues in this region (*25*). These receptors can now be tested to measure the effects of naturally occurring sequence variations on ligand sensitivity. Such a program, coupled with introduced mutations, could lead to a detailed, experimentally testable understanding of the relation between gene sequence, protein structure, and ligand-binding specificity in membrane-bound receptors.

REFERENCES AND NOTES

1. H. Breer, *Semin. Cell Biol.* **5**, 25 (1994); G. M. Shepherd, *Neuron* **13**, 771 (1994).
2. L. Buck and R. Axel, *Cell* **65**, 175 (1991).
3. D. Lancet and N. Ben-Arie, *Curr. Biol.* **3**, 668 (1993).
4. We assume here from previous in situ hybridization studies that each of the approximately 1000 receptors is expressed in roughly 0.1% of the total olfactory neurons [K. J. Ressler, S. L. Sullivan, L. B. Buck, *Cell* **73**, 597 (1993); R. Vassar, J. Ngai, R. Axel, *ibid.* **74**, 309 (1993)], so that if expression of one particular receptor could be induced in as few as 1 to 10% of the neurons, the additional response attributable to activation of that receptor by its particular ligands would be relatively easy to detect.
5. D. Ottoson, *Acta Physiol. Scand.* **35**, 1 (1956); *Handbook of Sensory Physiology (Olfaction)* (Springer-Verlag, Berlin, 1971), vol. 4, pp. 95–131; A. Mackay-Sim and S. Kesteven, *J. Neurophysiol.* **71**, 150 (1994).
6. F. L. Graham and L. Prevec, *Methods Mol. Biol.* **7**, 109 (1991); T. C. Becker *et al.*, in *Protein Expression in Animal Cells*, M. G. Roth, Ed. (Academic Press,

San Diego, CA, 1994), pp. 162–189; M. A. Rosenfeld *et al.*, *Cell* **68**, 143 (1992); J. Zabner *et al.*, *ibid.* **75**, 207 (1993); G. Le Gal Le Salle *et al.*, *Science* **259**, 988 (1993); K. Moriyoshi, L. J. Richards, C. Akazawa, D. D. M. O'Leary, S. Nakanishi, *Neuron* **16**, 255 (1996); A. J. G. D. Holtmaat *et al.*, *Mol. Brain Res.* **41**, 148 (1996).

7. The adenoviral vector AdexCAG-I7-IRES-GFP (Ad-I7) was constructed in the following manner. Adenoviruses lacking the E1 region of their genome are replication-incompetent and are grown in the complementary human embryonic kidney (HEK) 293 cell line, which provides the E1 genes in trans. The entire coding sequence for the rat odorant receptor I7 (*2*) was amplified by the polymerase chain reaction (PCR) using Pfu DNA polymerase (Stratagene) from the I7 clone plasmid with the upstream primer 5′-CCCTCGAGTATGGAGCGAAGGAACCAC-3′ and the downstream primer 5′-GCTCTAGACTAAC-CAATTTTGCTGCCT-3′. The 0.6-kb IRES (*9*) fragment was cut with Eco RI and Bam HI from plasmid p1162. The fragments of I7, IRES, and the S65T mutant of GFP were first conjugated in the multicloning sites of the expression vector pCA4 (Microbix, Ontario, Canada) and tested by Northern blot with a I7 probe for transcription of mRNA, and by green fluorescence for IRES-driven GFP expression in HEK 293 cells (ATCC, CRL-1573). The I7-IRES-GFP sequence was then subcloned into the Swa I site of the cosmid vector pAdex1pCAw (*26*) [Y. Kanegae *et al.*, *Nucleic Acids Res.* **23**, 3816 (1995)] to create the cosmid vector pAdexI7-IRES-GFP. The pAdex1pCAw cosmid was created from the human adenovirus type 5 genome from which the E1a, E1b, and E3 regions were deleted and replaced with an expression unit containing the CAG promoter, composed of the cytomegalovirus enhancer plus the chicken β-actin promoter [H. Niwa, K. Yamamura, J. Miyazaki, *Gene* **108**, 193 (1991)], a Swa I site, and the rabbit β-globin polyadenylation signal. The I7 sequence was confirmed by sequencing. Nucleotide 104 in the I7 sequence from GenBank (accession number M64386) is undefined. This nucleotide is deoxycytidine according to our sequence analysis; therefore, amino acid 35 in the deduced protein sequence is alanine. The cosmid vector pAdexI7-IRES-GFP and the Eco T22I–digested DNA-terminal protein complex (DNA-TPC) of Ad5-dlX, which is a human type 5 adenovirus lacking the E3 region, were cotransfected into HEK293 cells by calcium phosphate precipitation. The recombinant adenovirus AdexCAG-I7-IRES-GFP was then generated by homologous recombination in the HEK 293 cells. The DNA-TPC method has been described in detail (*26*) [S. Miyake *et al.*, *Proc. Natl. Acad. Sci. U.S.A.* **93**, 1320 (1996)]. Bam HI and Xba I digestion of the genomic DNA of AdexI7-IRES-GFP produced the appropriate band pattern, and positive PCR amplification of I7 also verified the construct. Because recombinant viruses do not include the E1a genes, PCR amplification of the E1a region was performed with the primers 5′-ATTACCGAAGAAATGGCCGC-3′ and 5′-CCCATTTAACACACGCCATGCA-3′, as a control for contamination by wild-type adenovirus (Ad5-dlX). Negative PCR amplification of the E1a gene was observed in every stock of recombinant adenovirus. The recombinant adenovirus was propagated in HEK 293 cells and purified by cesium gradient centrifugation [Y. Kanegae, M. Makimura, I. Saito, *Jpn. J. Med. Sci. Biol.* **47**, 157 (1994)]. The viral titer was determined by plaque-forming assay on HEK 293 cells.
8. The production of other viral proteins is also hindered because the E1 genes provide an essential function as transcriptional activators [T. Shenk, in *Fields Virology*, B. N. Fields *et al.*, Eds. (Lippincott-Raven, Philadelphia, 1996), vol. 2, pp. 2111–2138]. In an earlier study using an adenovirus vector containing the *lacZ* marker gene, we observed strong but heterogeneous viral infection and protein expression in rat nasal epithelium, and no virally induced cell loss out to 21 days after infection [H. Zhao, J. M. Otaki, S. Firestein, *J. Neurobiol.* **30**, 521 (1996)].
9. D. G. Kim, H. M. Kang, S. K. Jang, H. S. Shin, *Mol. Cell. Biol.* **12**, 3636 (1992).
10. Rats (Sprague-Dawley) of various ages and both sexes were used for these experiments. Under anesthesia (ketamine, 90 mg/kg, and xylazine,10 mg/kg, intraperitoneally), 30 μl of rat Ringer solution [135 mM NaCl, 5 mM KCl, 1 mM $CaCl_2$, 4 mM $MgCl_2$, and 10 mM Hepes (pH 7.4)] containing the virus at a titer of 3×10^9 pfu/ml and 0.3% fast green dye was slowly injected through the nostril into the right side of the nasal cavity with a thin plastic tubing. The solution was allowed to remain in the nasal cavity. After recovery, the animals were maintained at room temperature with no other treatment until they were killed.
11. Northern blot for detection of I7 mRNA was performed using a standard procedure [J. Sambrook, E. F. Fritsch, T. Maniatis, *Molecular Cloning: A Laboratory Manual* (Cold Spring Harbor Laboratory Press, Cold Spring Harbor, NY, 1989)]. Total RNAs were extracted from tissues with TRIzol reagent (Gibco-BRL); 20 μg of total RNA was loaded on each lane of the gel. The I7 probe was synthesized by PCR with primers that covered the entire I7 coding sequence and was labeled with digoxigenin (DIG-11-dUTP, Boehringer Mannheim) according to the manufacturer's protocol. After hybridization, the probe was detected with the DIG Nucleic Acid Detection Kit (Boehringer Mannheim).
12. G. Lowe and G. H. Gold, *Nature* **366**, 283 (1993).
13. The olfactory turbinates were dissected out, fixed with 4% paraformaldehyde in phosphate-buffered saline (PBS, pH 7.4) for 2 hours, and cryoprotected in 20% sucrose. Cryostat sections (15 μm) were cut and incubated with polyclonal antibody to GFP (Clontech). Specific staining was then visualized with the Vectastain Elite ABC kit (Vector Lab).
14. A panel of 74 odors were screened. They included odors from several classes and groups:

	Aromatics
Alcohols	Cinnamyl alcohol, eugenol, guaiacol
Aldehydes	*para*-Anisaldehyde, (−)-carvone, cinnamaldehyde, salicylaldehyde, lilial
Esters	Cinnamylformate, geranyl acetate, isoamyl salicylate, linalyl formate
Ethers	Anisole, cineole, 2-methylanisole, 4-methylanisole, isoeugenol, methyl eugenol
Heterocycles	2-Isobutyl-3-methoxypyrazin
Hydrocarbons	2-Ethyltoluene, 3-ethyltoluene, 1,2-diethylbenzene, limonen
Ketones	Acetophenone, 2-decalone
	Aliphatics
Alcohols	*n*-Propyl alcohol, *n*-butyl alcohol, *n*-pentyl alcohol, *n*-hexyl alcohol, *n*-heptyl alcohol, *n*-octyl alcohol, *n*-nonyl alcohol, *n*-decyl alcohol, 2-ethylfenchol, geraniol, β-citronellol, linalool
Aldehydes	Propion aldehyde, isobutyraldehyde, *n*-valeraldehyde, *n*-hexaldehyde, *n*-heptaldehyde, *n*-octyl aldehyde, *n*-nonyl aldehyde, *n*-decyl aldehyde, undecylic aldehyde, dodecyl aldehyde, *trans*-2-octenal, 2-octynal, *trans*-2-tridecanal, citral, lyral
Acids	Propionic acid, *n*-valeric acid, *n*-octanoic acid, *n*-nonanoic acid
Alkanes	*n*-Octane, *n*-nonane, *n*-decane
Amines	Isopentylamine, phenethylamine
Esters	Amyl acetate, ethyl butyrate, ethyl hexanoate, isoamyl acetate, octyl butyrate, octyl isovalerate
Ethers	Citral diethyl acetal, citral dimethyl acetal
Ketones	2,3-Butanedione, 1-fenchone, 2-nonanone
Other	Heptyl cyanide, 1,1,3,3-tetramethylbutyl isocyanide

15. Odorant solutions were prepared as 0.5 M stocks in dimethyl sulfoxide (DMSO) and were then diluted with water to the concentration for EOG recording. All odorants were prepared at a liquid concentration of 10^{-3} M; those with low volatilities were additionally prepared at 10^{-2} M. At 10^{-3} M the DMSO concentration in solution was 0.2% (v/v). Responses to DMSO alone were the same as to clean air (that is, <0.5 mV). All odorant chemicals were purchased from Aldrich except lyral and lilial, provided by IFF and Harmon & Reimer Inc. A 3-ml sample of the odorant solution was placed in a 10-ml glass test tube and capped with a silicon stopper. The concentration of volatile odorant in the 7-cm^3 airspace was allowed to equilibrate for more than 1 hour. All solutions were used within 8 hours. Two 18-gauge needles provided the input and output ports for the odorant-containing vapor above the solution. For stimulation, a 100-ms pulse of the odorant vapor at 9 psi was injected into the continuous stream of humidified air. The pulse was controlled by a Picospritzer solenoid-controlled valve (General Valve). The odorant stimulus pathway was cleaned by air between each stimulus presentation. The minimum interval between two adjacent stimuli was 1 min.
16. The animal was overdosed with anesthetics (ketamine and xylazine) and decapitated. The head was cut open sagitally and the septum was removed to expose the medial surface of the olfactory turbinates [S. G. Shirley, E. H. Polak, D. A. Edwards, M. A. Wood, G. H. Dodd, *Biochem. J.* **245**, 185 (1987)]. The right half of the head was mounted in a wax dish filled with rat Ringer solution. The medial surface of turbinates was face up and exposed to the air. A continuous stream of humidified clean air was gently blown on the turbinates through tubing to prevent tissue from drying. The opening of the tubing was 8 mm in diameter and was placed about 10 mm from the turbinate surface. The EOG recording electrode was an Ag-AgCl wire in a capillary glass pipette filled with rat Ringer solution containing 0.6% agarose. The electrode resistance was 0.5 to 1 megohm. The recording pipette was placed on the surface of the olfactory epithelium and connected to a differential amplifier (DP-301, Warner Instruments). Placement of the electrode was determined by visualizing GFP fluorescence with a modified stereomicroscope (Kramer Scientific). The EOG potential was observed on a chart recorder, recorded with a digital audio tape recorder, and later transferred to computer. For most experiments, two electrodes and two amplifiers were used to record EOGs from two different sites of epithelium simultaneously. All experiments were performed at room temperature (22° to 25°C).
17. Because of interanimal variability in the responses to the large number of odors used, we adopted a normalization strategy to facilitate comparisons. All responses within an individual animal were normalized to the response to a standard odor, amyl acetate. The peak amplitude of the amyl acetate response was always given the value of 1, and all other responses are represented as a percentage of the amyl acetate response. Amyl acetate was chosen because it typically gives a large, robust, and repeatable response. The amyl acetate responses varied from 2 to 15 mV over the entire sample size. The same procedures were used on data from uninfected, Ad-I7–infected, and control-infected animals. To account for the temporal variability over the course of a 2- to 3-hour experiment, the amyl acetate standard was delivered on every sixth trial and intervening responses were normalized to the average of the preceding and following amyl acetate responses. Three tubes of amyl acetate at a solution concentration of 10^{-3} M were used alternately in each experiment.
18. Epithelia were dissociated as described [D. Restrepo, M. M. Zviman, N. E. Rawson, in *Experimental Cell Biology of Taste and Olfaction*, A. I. Spileman and J. G. Brand, Eds. (CRC Press, Boca Raton, FL, 1995), pp. 387–398]. Whole-cell recordings were made with an Axopatch 1D amplifier (Axon Instruments); data were acquired and analyzed with HEKA Pulse software. Electrode pipettes had a resistance of 5 to 10 megohms and contained 135 mM CsCl, 1

mM $CaCl_2$, 1 mM $MgCl_2$, 10 mM EGTA, 10 mM Hepes, 4 mM adenosine triphosphate, and 0.3 mM guanosine triphosphate (pH 7.4). Cells were bathed in a solution of 138 mM NaCl, 5 mM KCl, 0.5 mM $CaCl_2$, 1.5 mM $MgCl_2$, 10 mM Hepes, and 10 mM glucose (pH 7.4). Odor stimuli were delivered with the SF77 Fast Perfusion system (Warner Instruments), allowing precise concentrations to be applied for steps of various durations.

19. Five animals were infected with virus containing only the *lacZ* gene. In each animal the EOG electrode was positioned in several areas over the epithelium. After recording, the epithelia were reacted with X-gal and 18 electrode positions were determined to have been within areas of high infection. Responses to octanal at those positions were not different from those of uninfected animals.
20. T. Sato, J. Hirono, M. Tonioke, M. Takebayashi, *J. Neurophysiol.* **72**, 2980 (1994). K. Mori and Y. Yoshihara, *Prog. Neurobiol.* **45**, 585 (1995).
21. K. Raming *et al.*, *Nature* **361**, 353 (1993).
22. P. Sengupta, J. H. Chou, C. I. Bargmann, *Cell* **84**, 899 (1996); Y. Zhang, J. H. Chou, J. Bradley, C. I. Bargmann, K. Zinn, *Proc. Natl. Acad. Sci. U.S.A.* **94**, 12162 (1997).
23. C. Wellerdieck *et al.*, *Chem. Senses* **22**, 467 (1997).
24. J. Ostrowski, M. Kjelsberg, M. Caron, R. Lefkowitz, *Annu. Rev. Pharmacol. Toxicol.* **32**, 167 (1992).
25. J. Ngai, M. M. Dowling, L. Buck, R. Axel, A. Chess, *Cell* **72**, 657 (1993).
26. M. Hashimoto *et al.*, *Hum. Gene Ther.* **7**, 149 (1996).
27. We thank K. Mikoshiba, E. Falck-Pedersen, M. Chao, and in particular S. O. Yoon for expert advice and assistance; L. Buck and H. Breer for receptor clones; T. Lufkin for the IRES construct; L. Richards and K. Moriyoshi for GFP adenovirus; IFF and Harmon & Reimer Inc. for lyral and lilial; Y. Huang for technical assistance; and R. Axel, D. Kelley, and P. Mombaerts for thoughtful comments. J.M.O. would like to dedicate this paper to the memory of Yoko Sakaki. This work was supported by the Whitehall and McKnight Foundations and the National Institute on Deafness and Other Communication Disorders.

23 September 1997; accepted 19 November 1997

Frameshift Mutants of β Amyloid Precursor Protein and Ubiquitin-B in Alzheimer's and Down Patients

Fred W. van Leeuwen,* Dominique P. V. de Kleijn, Helma H. van den Hurk, Andrea Neubauer, Marc A. F. Sonnemans, Jacqueline A. Sluijs, Soner Köycü, Ravindra D. J. Ramdjielal, Ahmad Salehi, Gerard J. M. Martens, Frank G. Grosveld, J. Peter H. Burbach, Elly M. Hol

The cerebral cortex of Alzheimer's and Down syndrome patients is characterized by the presence of protein deposits in neurofibrillary tangles, neuritic plaques, and neuropil threads. These structures were shown to contain forms of β amyloid precursor protein and ubiquitin-B that are aberrant (+1 proteins) in the carboxyl terminus. The +1 proteins were not found in young control patients, whereas the presence of ubiquitin-B^{+1} in elderly control patients may indicate early stages of neurodegeneration. The two species of +1 proteins displayed cellular colocalization, suggesting a common origin, operating at the transcriptional level or by posttranscriptional editing of RNA. This type of transcript mutation is likely an important factor in the widely occurring nonfamilial early- and late-onset forms of Alzheimer's disease.

In Alzheimer's disease (AD) and Down syndrome (DS) patients, intracellular and extracellular deposits of proteins in tangles, neuropil threads, and neuritic plaques are correlated with neuronal dysfunction leading to dementia (*1*). In particular, the familial types of AD have been investigated thoroughly and are due to mutations in genes located on chromosomes 1, 14, and 21, and the apolipoprotein E genotype (chromosome 19) is a risk factor (*2*). However, at least 60% of AD patients do not have a family history of the disease (*3*). For these frequently occurring, sporadic cases, a more general mechanism must exist, ultimately leading to neuronal degeneration.

Messenger RNA editing is a means of producing phenotypic variability (*4*). Moreover, we have identified another type of mutation in vasopressin transcripts (*5*). Homozygous Brattleboro rats have a single base deletion in the vasopressin gene, and newborn rats do not have a functional vasopressin mRNA and protein. Surprisingly, functional RNA and protein are found in a small but increasing proportion of hypothalamic cells as the animals age (*6*). This apparent reversion is due to a dinucleotide deletion (ΔGA) within GAGAG motifs of the mutant RNA (*5*). Thus, genetic information in neurons is not stable but subject to modification through an as yet unknown mechanism. We surmised that the opposite process may take place in other neuronal genes, resulting in mutant transcripts from wild-type genes, and so we looked for dinucleotide deletions in two genes associated with the pathogenesis of AD. The genes encoding β amyloid precursor protein (βAPP) and ubiquitin-B (Ubi-B) protein (*1*, *7*) each contain several GAGAG motifs.

In βAPP mRNA, seven GAGAG motifs are present in regions corresponding to exons 4, 6, 9, 10, and 14. Because three motifs are clustered in exons 9 and 10, this part of the transcript, encoding a putative growth-promoting domain (*8*), was selected for the detection of a +1 frameshift mutation resulting in truncated βAPP (βAPP^{+1}) with a novel COOH-terminus (Fig. 1A). In two of the three repeats of Ubi-B mRNA, a single GAGAG motif is present (Fig. 1A). The predicted +1 frameshift results in an aberrant COOH-terminus of Ubi-B of the first or second repeat (Ubi-B^{+1}). As a result, the glycine moiety essential for multiubiquitylation (*9*) would be lacking. To examine the occurrence of the predicted +1 proteins, we generated antibodies to the novel COOH-termini of βAPP^{+1} and Ubi-B^{+1} and used them to evaluate the presence of the abnormal proteins in tissue sections of cerebral cortex from AD, DS, and control patients by immunocytochemistry (*10*) and immunoblot analysis (*11*) and to assess reading frame mutations by selecting cDNA clones expressing +1 immunoreactivity.

Immunoreactivity for βAPP^{+1} and Ubi-B^{+1} was prominent in early- and late-onset AD cases and even more prominent in DS patients compared with controls matched for age, sex, postmortem delay, and duration of fixation (*12*) (Fig. 2 and Table 1). When the three brain areas studied were taken together, βAPP^{+1} immunoreactive structures were present in 71% and Ubi-B^{+1} immunoreactive structures in 100% of the AD patients (*12*). In young controls and one nondemented DS patient devoid of neuropathology in the frontal and temporal cortices and hippocampus, no Ubi-B^{+1} immunoreactivity was found (*12*). When Ubi-B^{+1} immunoreactivity was found in elderly, nondemented controls (>72 years), their neuropathological diagnosis revealed the presence of some plaques and tangles (*12*). Furthermore, no βAPP^{+1} and Ubi-B^{+1} immunoreactivities were found in the substan-

F. W. van Leeuwen, D. P. V. de Kleijn, A. Neubauer, M. A. F. Sonnemans, J. A. Sluijs, S. Köycü, R. D. J. Ramdjielal, A. Salehi, E. M. Hol, Graduate School for Neurosciences Amsterdam, Netherlands Institute for Brain Research, 1105 AZ Amsterdam, Netherlands.
H. H. van den Hurk and G. J. M. Martens, Department of Molecular Animal Physiology, University of Nijmegen, 6525 ED Nijmegen, Netherlands.
F. G. Grosveld, Department of Cell Biology and Genetics, Erasmus University, 3000 DR Rotterdam, Netherlands.
J. P. H. Burbach, Rudolf Magnus Institute for Neurosciences, 3584 CG Utrecht, Netherlands.

*To whom correspondence should be addressed. E-mail: f.van.leeuwen@nih.knaw.nl